JOURNAL OF BACTERIOLOGY, Oct. 2000, p. 5925–5930 Vol. 182, No. 20
0021-9193/00/$04.00+0

On the Architecture of the Gram-Negative Bacterial Murein Sacculus

DAVID PINK,[1]* JEREMY MOELLER,[1] BONNIE QUINN,[1] MANFRED JERICHO,[2] AND TERRY BEVERIDGE[3]

TPI, Physics Department, St. Francis Xavier University, Antigonish, Nova Scotia, Canada B2G 2W5,[1] Department of Microbiology, College of Biological Science, University of Guelph, Guelph, Ontario, Canada N1G 2W1,[3] and Physics Department, Dalhousie University, Halifax, Nova Scotia, Canada B3H 4J1[2]

Received 27 March 2000/Accepted 18 July 2000

The peptidoglycan network of the murein sacculus must be porous so that nutrients, waste products, and secreted proteins can pass through. Using *Escherichia coli* and *Pseudomonas aeruginosa* as a baseline for gram-negative sacculi, the hole size distribution in the peptidoglycan network has been modeled by computer simulation to deduce the network's properties. By requiring that the distribution of glycan chain lengths predicted by the model be in accord with the distribution observed, we conclude that the holes are slits running essentially perpendicular to the local axis of the glycan chains (i.e., the slits run along the long axis of the cell). This result is in accord with previous permeability measurements of Beveridge and Jack and Demchik and Koch. We outline possible advantages that might accrue to the bacterium via this architecture and suggest ways in which such defect structures might be detected. Certainly, large molecules do penetrate the peptidoglycan layer of gram-negative bacteria, and the small slits that we suggest might be made larger by the bacterium.

Bearing in mind that a thorough knowledge of structure can lead to an understanding of function, it is important to elucidate the detailed molecular structures of bacterial surfaces. There have been few recent studies of the physical properties of murein sacculi (12, 18, 20), and yet this cell wall component is of paramount importance to the integrity of the cell. It must have high tensile strength and at the same time be highly permeable to nutrients, waste products, and secreted proteins. Even large macromolecules such as DNA (in genetic exchange, such as transformation) and S-layer proteins can pass through (1, 17). The murein of a gram-negative bacterium is composed of one to three layers of peptidoglycan (12, 19) and is bonded via lipoprotein moieties to the outer membrane; these can be either covalently or electrostatically attached to the peptidoglycan (1). Our recent work on the elasticity and thickness of *Escherichia coli* and *Pseudomonas aeruginosa* murein sacculi has helped define several physical properties of this intriguing cell wall fabric (20), but the work did not elucidate the network's porosity. Since 35 to 50% of the peptide stems of peptidoglycan are cross-linked at a given time in the cell's growth cycle (5, 7), this bonding between neighboring glycan strands should be important not only for the fabric's ability to withstand physical strain but also for its porosity. Indeed, it could even be possible for this limited cross-linking in combination with the finite length of each glycan strand to form peptidoglycan arrangements such that holes of various kinds occur within the network. Because of the dynamic nature of cell growth and peptidoglycan turnover, these holes could be transient and difficult to find, especially since they would be at nanoscale dimensions. Yet, the question of holes in these networks is of fundamental importance, and here we resort to computer modeling to predict their existence and distribution. A knowledge of the shape and size distributions of such holes, as well as the variances in these distributions, can be relevant for understanding the passage of molecules through the peptidoglycan layer, the elasticity of the layer, and, possibly, aspects of the mechanics of cell division. In this note, we show the expected distribution of holes deduced from the distribution of glycan strand lengths (5, 7, 9) and discuss their possible consequences for the viability of the bacterium.

Peptidoglycan chemical structure and initial discussion of holes in a monomolecular thick peptidoglycan network. There can be two types of cross-linkages occurring between adjacent glycan strands in a peptidoglycan network: cross-links that occur somewhere in the middle region of a glycan strand and those that occur at the terminus of a strand. Since each peptidoglycan strand possesses a screw axis, the peptide stems are helically arranged so that they protrude at ~90° to one another (7, 11). Accordingly, only a maximum of 50% of the stems can be cross-linked in a horizontal plane. At that point, the network exhibits maximum cross-linking. Frequently, each cross-link involves a covalent bond between a 3-amino-acid stem and a 4-amino-acid stem (L-Gla–D-Glu–*m*-A_2pm–D-Ala—*m*-A_2pm–D-Glu–L-Ala) or between two 4-amino-acid stems (L-Ala–D-Glu–*m*-A_2pm–D-Ala—*m*-A_2pm [D-Ala]–D-Glu–L-Ala), each emanating from adjacent *N*-acetylmuramyl moieties on neighboring glycan strands (i.e., a septapeptide or an octapeptide cross-link). Whenever a cross-link involves a 4-amino-acid stem (L-Ala–D-Glu–*m*-A_2pm–D-Ala) and a 5-amino-acid stem (L-Ala–D-Glu–*m*-A_2pm–D-Ala–D-Ala; i.e., the terminal D-Ala has not been cleaved by the D,D-carboxypeptidase), the linkage is referred to as a nonapeptide cross-link. The parts of the peptide stems that proceed beyond each cross-link are not stressed by the bacterium's turgor pressure. If all glycan strands were much longer than the typical septapeptide, octapeptide, or nonapeptide cross-links and if the maximum possible number of these cross-links had been produced in a peptidoglycan network, i.e., if 50% of the peptide stems are cross-linked, then all the holes in the network would be essentially the same size. This size is the area bounded by two successive cross-links and the two intervening sections of glycan strands, as shown in Fig. 1A. Figure 1B shows a representation of a network which is maximally cross-linked, thus possessing the smallest possible holes. We have not shown the possibility that these smallest holes become approximately hexagonal when the network is stretched (10)—we are not immediately concerned with what

* Corresponding author. Mailing address: TP1, Physics Department, St. Francis Xavier University, P.O. Box 5000, Antigonish, Nova Scotia, Canada B2G 2W5. Phone: (902) 837-3987. Fax: (902) 867-2414. E-mail: dpink@stfx.ca.

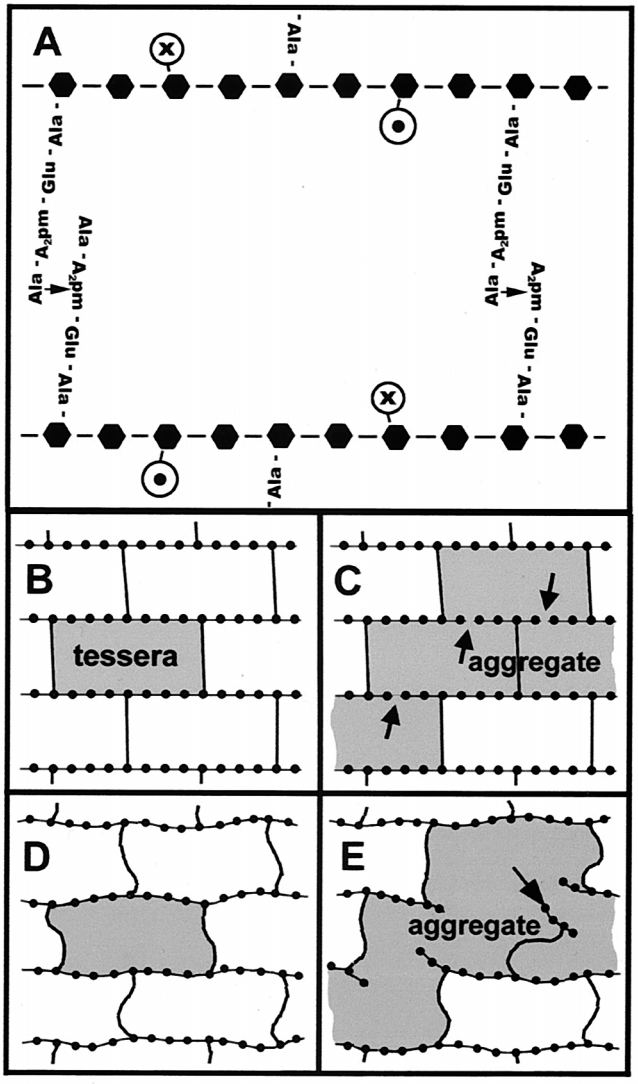

FIG. 1. (A) Diagram of a portion of a murein sacculus. The hexagons represent the *N*-acetylglucosamine and the *N*-acetylmuramic acid (Mur) groups. Two complete cross-links are shown attached to the latter. One is a nonapeptide link (left), while the other is an octapeptide link (right). Circles containing ● or × indicate unlinked pentapeptide groups, attached to Mur groups and oriented out of or into the plane. (B and D) Diagram of infinitely long glycan strands (horizontal) maximally cross-linked via nonapeptide or octapeptide chains. A tessera is shown shaded. The dots represent the sugar groups along the glycan strands. (D) Effect of temperature-driven fluctuations in this elastic system. (C and E) The peptidoglycan network of A with six glycan strand ends shown (arrows) giving rise to an aggregate of four tesserae (shaded). The hexagonal structure is not represented here. (E) Effect of temperature-driven fluctuations in this elastic system. The arrow points to a small, attached but isolated peptidoglycan remnant that is relatively free to move. Note the possibility of opening a large hole in the sacculus.

shape the holes adopt in a bacterium, since it is possible that the cell might exert local forces, thereby additionally distorting its peptidoglycan network (following Koch, we call these smallest holes tesserae [i.e., units having four corners]). In reality, however, the glycan strands are not very much longer than the cross-links but range from 2 to over 30 disaccharides long (5, 7, 9, 14), so it is possible that one of the intervening sections of a glycan strand bounding a tessera appears broken. Instead of one continuous glycan strand, the network at this point is composed of the ends of two different glycan strands. In this case, two adjacent tesserae are actually connected, thereby creating an aggregate (of tesserae) formed by two connected tesserae (Fig. 1C shows four such connected tesserae). An assumption will be made that there are minimal gaps between the ends of two abutting glycan strands, as shown in Fig. 1C. This assumption is justified by the observation that, in *E. coli* and *P. aeruginosa*, 50% of the pentapeptide strands form cross-links. If gaps existed between the ends of abutting glycan chains, then some unlinked peptapeptide chains lying in the plane of the network would lack another pentapeptide partner from an adjacent strand with which to form a cross-link. Finally, Fig. 1D and E show how the networks of Fig. 1B and C might behave at higher temperatures, where high-energy thermal oscillations give rise to distortions of the network. The network containing the aggregate (Fig. 1C) undergoes even larger distortions than that containing only tesserae because of the proximity of many glycan strand ends, which lead to the opening of a large hole in the lattice. It will be shown below that, in a monomolecular thick peptidoglycan network, it is possible to deduce the general form of the distribution of the holes, their general shape, and their alignment to one another from a knowledge of the distribution of glycan strand lengths.

Mathematical models and techniques. To explore the size distribution of holes in a peptidoglycan network formed from a set of glycan strands exhibiting a distribution of lengths, we considered trying to assemble the glycan strands in some manner, possibly random. This proved difficult, because it became apparent that when choosing a particular strand and a place to insert it, we had to be aware of the existing structure of the local network; otherwise, the fabric could be left with large gaps between the ends of successive strands. The use of Monte Carlo techniques to anneal a structure containing such gaps could be very time-consuming and would not necessarily solve the problem. This procedure of inserting glycan strands into a preexisting peptidoglycan network is performed by bacteria, as they (somehow) determine exactly where each piece should go, but we do not know the rules they are following. Accordingly, we solved this problem by cutting otherwise very long glycan strands so that the procedure resulted in the experimentally observed glycan strand length distribution. Cutting the strands of a network is a standard technique in the simulation of percolation and has been applied in a biological context (references 15 and 16 and references therein). That application, however, was without any analogue of the requirement here, i.e., that the resulting glycan chain length distribution must be in accord with experimental results. In that application, also, all bonds could be cut, leading to the possibility that sections of the network could be separated from the main body (15) (Fig. 1). Our model does not permit this, and we comment on this below.

We began with a flat plane, with periodic boundary conditions, composed of glycan strands possessing no breaks, and we assumed maximum cross-linking (see above). The glycan strands were laid down parallel to each other with the maximum number of pentapeptide chains in register. This allowed the maximum number of cross-links, formed from pairs of nearest-neighbor pentapeptides, to be created, yielding a peptidoglycan network that contained only tesserae (Fig. 2A). We then introduced the concept of an "aggregate of size *s*," defined as a set of *s* tesserae which are connected by having the ends of glycan strands in common. Each aggregate of size *s* was created by a rule, B, which defined a sequence of breaks in the glycan strands that permitted *s* tesserae to be connected. Such an aggregate can be created in a variety of ways, but with one constraint: the breaks in the glycan strands may not isolate a portion of the peptidoglycan network so that it becomes disconnected from the remainder of the network. There is no experimental reason for this constraint except that, should a

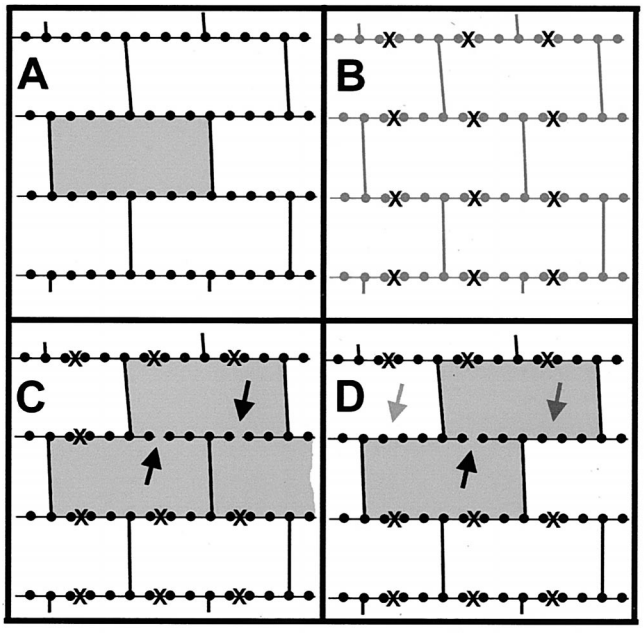

FIG. 2. (A) Diagram of infinitely long glycan strands (horizontal) maximally cross-linked via nonapeptide or octapeptide chains. A tessera is shown shaded. (B) The peptidoglycan system of panel A. The locations where the glycan strands may be cut are indicated by ×s. (C) Construction of an aggregate according to rule B1. The glycan chain has been cut in two places (dark arrows), and the three tesserae thus connected are shaded. (D) Illustration of rule B2. With the glycan chain cut at the dark arrow, the two ×s on either side of the cut (light arrows) have been removed to show that those sites may not be cut. The solid circles represent sugar groups along the glycan strands.

section of the peptidoglycan network become disconnected from the remainder of the network, the structure would be weakened. There appears to be no obvious advantage for a bacterium in adopting such a structure. In order to actually construct a set of aggregates, it is clearly necessary that a size distribution, $D_s(s)$, which yields the fraction of aggregates composed of s tesserae be specified.

This set of aggregates, represented by the distribution $D_s(s)$, was distributed, according to a rule H, on the plane of the peptidoglycan network. Bearing in mind that aggregates introduce breaks in the glycan chains, the network was now composed of a distribution of finite-length glycan chains. The length distribution, $D_L(L)$, yielding the fraction of glycan strands of length L, could then be calculated and compared to the results of the experiment. In what follows, we present the rationale for different choices of $D_s(s)$ and rule H and the results.

Creation of holes. The following procedure was used to create a set of aggregates possessing a size distribution $D_s(s)$. First, we selected the total number of aggregates we wanted produced and then selected a size, s, in accord with the probability, $D_s(s)$, that such a size would occur in the distribution. An aggregate of size s was then created as follows. We assumed, for simplicity, that the two glycan strands bordering a tessera could be cut at four sites, and their locations are identified in Fig. 2B. We selected one of these sites randomly but in accord with rules B1 and B2 (see below) and, by cutting there, attached a second tessera to the first tessera. The two-tessera aggregate thus created possessed five sites at which it was possible to cut. We then randomly chose one of the two tessera as well as a site on one of its glycan strands at which to cut. By cutting at that site, a third tessera was attached to the growing aggregate. This procedure is shown in Fig. 2C, where the two cuts that create the three-tessera aggregate are indicated. The procedure terminated when sufficient cuts had been performed to create an s-tessera aggregate. The resulting structure was then placed anywhere convenient on the maximally cross-linked peptidoglycan network.

(i) Rules B1 and B2. Rules B1 and B2 dealt with the procedures used to select sites on the glycan chains at which to cut. We began by imposing no conditions on which sites (Fig. 2B) we could cut at (rule B1) but with the condition that, as the aggregates were constructed, they were not cut in such a way as to cause a section of the network to become separated from the remainder of the network. For reasons to be described below, we also introduced rule B2. This states that, if a cut was made at a site, then cuts could not be made at the sites nearest to it along the same glycan strand and belonging to the same tessera. This is shown in Fig. 2D, where the cut is indicated and the two sites where cuts were not permitted in any future operation are also shown.

The set of aggregates of various shapes, exhibiting a size distribution $D_s(s)$, now distributed on the peptidoglycan network, resulted in a distribution of glycan strand lengths $D_L(L)$. We then moved the aggregates around, according to rule H (see below), until $D_L(L)$ had achieved a steady-state distribution.

(ii) Rule H. There are many ways to mimic what a bacterium might be doing without suggesting that this is the method that it actually uses. In the mathematical model used here, we moved the aggregates on the plane of the network subject to an interaction, V, which determined their average spatial distribution. We are unaware of how a bacterium actually controls the distribution of glycan strand ends. Our intent was simply to discover whether it does so, and we achieved this by introducing the effective interaction, V, which was parameterized by an interaction strength, V_0, between pairs of aggregates. If V_0 was positive (negative), then the interaction between pairs of aggregates was repulsive (attractive). Choosing a V_0 equal to 0 would result in a random distribution, as long as the density of aggregates was not too high (i.e., as long as the aggregates could find sufficient room between the other aggregates to move around). It should be clear that the aggregates do not rotate—they undergo only lateral movement. Since the bacterium probably does not create glycan chain lengths by using our mathematical procedure, our interaction, V, might not be easily identified with parameters of the procedure actually used by the bacterium. The analytical form used for V is given in the appendix.

We used the following two choices for the functional form of $D_s(s)$, the distribution aggregate sizes:

$$D_s(s) = A\exp(-[s_0 - s]^2/\Gamma^2) \quad (1a)$$

$$D_s(s) = 1 \text{ if } s = s_0 \quad (1b)$$

$$= 0 \text{ if } s \neq s_0$$

where A is an amplitude chosen so that the sum over s is equal to unity. In equation 1a, the bacterium would have distributed glycan strand lengths leading to a gaussian (normal) distribution of aggregate sizes, with an average size (aggregates composed of s_0 tesserae each) and a range of sizes (variance determined by Γ^2). The second distribution, equation 1b, would arise if the bacterium had distributed glycan strand ends which resulted in all aggregates being the same size, each containing s_0 tesserae. These two possibilities cover two extremes from which we might learn about the actual distribution in gram-negative bacteria.

In order to move the aggregates on the network, we made use of Monte Carlo techniques using the energy function (see

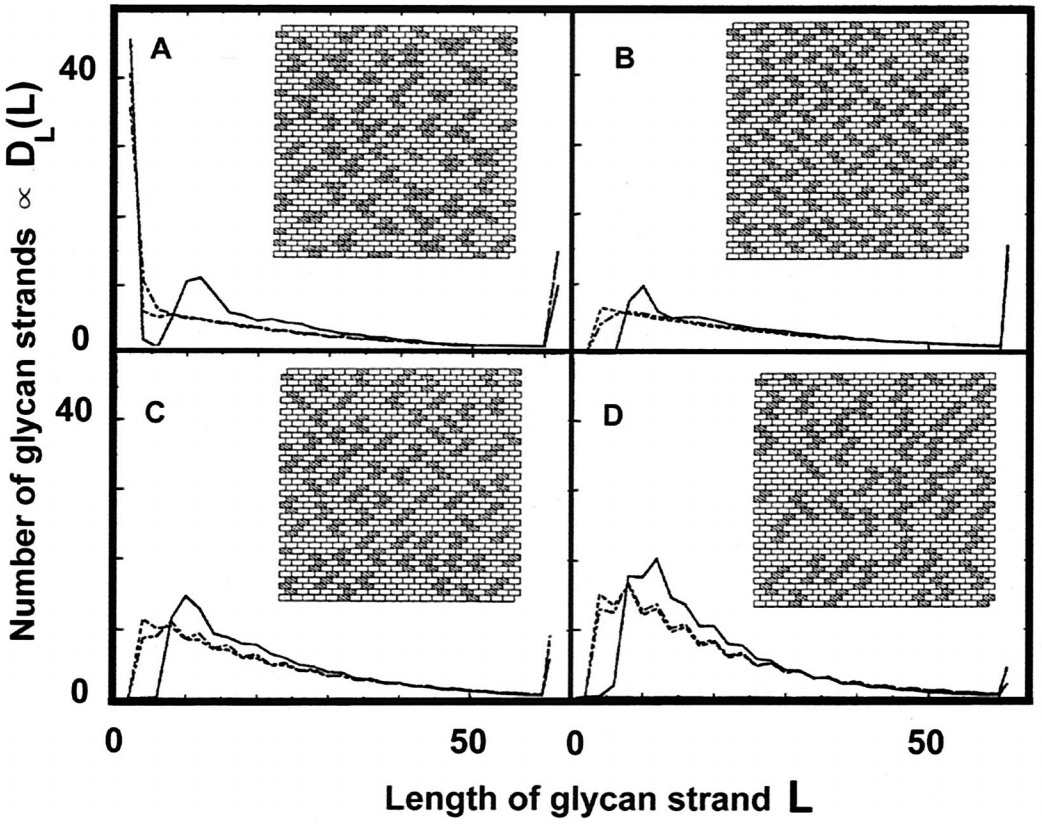

FIG. 3. $D_L(L)$, the fraction of glycan strands possessing length L, as a function of glycan strand length L, for different values of repulsive potential V_0. The dashed lines indicate a V_0 of 0 (short dashes) and a V_0 of 2. The solid lines indicate a V_0 of 5. At an L of 61, the curve indicates the sum of all values of $D_L(L)$ for an L of >60. The insets show typical distributions of aggregates for a V_0 of 5. (A) Use of rule B1. $D_s(s)$ is gaussian, with s_0 equal to 4 and Γ equal to 2. (B to D) Use of rule B2 to eliminate short glycan strands. $D_s(s) = 1$ for $s = s_0$ and $D_s(s) = 0$ for $s \neq s_0$; otherwise all aggregates possess the same number of tesserae. (B) $s_0 = 2$; (C) $s_0 = 3$; (D) $s_0 = 5$.

equation in the appendix). We used the Metropolis algorithm (4) with the magnitudes of V_0 and distance chosen so that aggregate moves were achieved for at least 50% of the attempts, with equilibrium achieved within a few thousand steps. We chose V_0 to be negative so as to keep the aggregates apart. The networks used initially contained 1,600 tesserae.

Results. Figure 3A shows glycan strand length distributions with 25% of the network covered by aggregates and utilizing rule B1 and a gaussian distribution with s_0 equal to 4 and Γ equal to 2. The graph shows the distribution of glycan strand lengths, $D_L(L)$, for V_0s of 0, 2, and 5, with an insert showing the distribution of aggregates for a V_0 of 5. These values were chosen with the intention of obtaining a glycan strand length distribution similar to that obtained by Obermann and Höltje (14). However, although $D_L(L)$ exhibits a local maximum at values of L corresponding to those observed by those authors when V_0 is equal to 5, there is a maximum at the shortest length, an L of 2. The maximum at the shortest glycan chain lengths is absent in the results of Obermann and Höltje. The reason for this was easily discovered. There are two ways of creating glycan chain lengths in our system. The first is controlled by the distribution of aggregates on the network, and this gives rise to a local maximum at the larger value of L. However, the large numbers of glycan strands with an L of 2 arise inside aggregates. They are created when cuts are made at adjacent sites, along the same glycan strand, on either side of a cross-link (Fig. 1C and E and 2C). Although we have no proof that we will necessarily obtain a maximum in $D_L(L)$ for an L of 2, we have been unable to find a counterexample that yields a maximum in accord with the results of Obermann and Höltje without another maximum at an L of 2. Obermann and Höltje (14) report that the number of strands of length (L) 2 is near zero. Because of this, we introduced rule B2 (see above), which states that if a cut was made at a site, then cuts could not be made at the sites nearest to it along the same glycan strand and belonging to the same unit (Fig. 2D).

Figure 3B to D shows results, using rule B2, for $D_L(L)$ with V_0s of 0, 2, and 5 obtained for the distribution of equation 1b with s_0s of 2, 3, and 5. The inserts show the distribution of the aggregates for a V_0 of 5. We now see that there is only one maximum in the chain length distribution and that there are no chains where L is equal to 2. The consequence of this is that the aggregates are now all slits running essentially perpendicular to the axis of the glycan strands. Although we cannot identify a distribution of aggregate sizes, it seems clear from our results that the slits are kept apart by the bacterium, as suggested by the experimentally observed form of $D_L(L)$. This is achieved in our model by means of an effective aggregate-aggregate repulsive interaction (see the appendix). The technique by which the bacterium might achieve this is not yet clear. Comparing the experimental results with the L dependence of $D_L(L)$ obtained by us suggests that s_0 is >5.

Conclusions. We have modeled the distribution of holes in the murein sacculus (peptidoglycan network) of gram-negative bacteria as represented by *E. coli* and *P. aeruginosa*. By requiring that the length distribution of glycan strands be in accord with the results of others (5, 7, 9, 14), we conclude that all the holes are slits running essentially perpendicular to the axis of

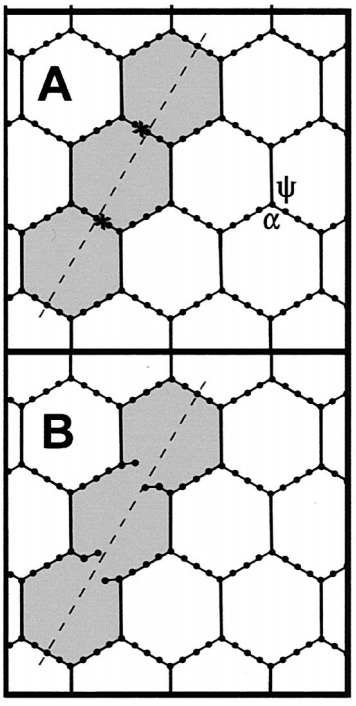

FIG. 4. (A) Turgor pressure-stretched peptidoglycan network such that the holes formed by the tesserae become hexagons. The cross-links at two peptide stem junctions are being cut at the regions marked by ×s to form a slit aggregate comprising three tesserae. (B) The network of A with the slit shown. It can be seen that although the slit is ~6 nm long, the lateral dimension will remain ~2 nm.

the glycan strands (Fig. 2D and 3B, C, and D). If the slits are not too large, then our results are in accord with what has been observed by Beveridge and Jack (2) and Demchik and Koch (6) regarding the permeability of bacterial walls. In addition, there appear to be some possible advantages to a distribution of slits as described here.

Demchik and Koch (6) measured the permeability of the wall fabric of *E. coli* and *B. subtilis* and concluded that the effective hole radius in these walls is slightly more than 2 nm. They pointed out that this is the characteristic dimension of a single tessera in the peptidoglycan network. If the slits are not too large, then our results are in accord with this, as illustrated in Fig. 4. There we have shown a network under tension, with an aggregate composed of three tesserae. It is clear that if the network is allowed to relax (not shown in Fig. 4B), then the characteristic dimensions of the slit are a length of ~6 nm and a width of ~2 nm. The limiting dimension here is the smaller one, so the passage of the molecules used by Demchik and Koch would be inhibited by slits as described here. This conclusion would not hold if aggregates of more general shapes were formed, as in Fig. 1E and 3A. There it can be seen that the interiors of larger aggregates, composed of segments similar to that in Fig. 1E, would have no means of inhibiting the entry of a molecule with a radius of >2 nm.

Consider a cylinder fabricated out of glycan strands, which adopt the zigzag conformation in an average direction perpendicular to the long axis of the cylinder, viz., the cell axis, with the octa- and nonapeptide cross-links oriented along the axis of the cylinder. In contrast to the many conformational states accessible by the cross-links, the glycan strands possess conformational freedom only via rotation around the oxygen linkages. Straightening the glycan strands would necessitate carrying out rotations of the sugar residues around those bonds. Certainly, gram-negative rods do not have much expansion around their girths (13), but the existence of slits of the kind described here distributed among the peptidoglycan network would allow more elasticity.

All peptidoglycan networks must be porous; otherwise, the free diffusion of nutrients and waste products could not occur. Furthermore, large secreted substances (e.g., S-layer proteins are typically 50 to 120 kDa [17]) are known to pass through. Of course, it is possible that large molecules are (somehow) linearized so that they can pass, but many periplasmic enzymes (previous to export) are functional, which implies they have correctly folded and are no longer completely linear. Slits (arising from rule B2) increase hole size, and it is possible that slits in the peptidoglycan alter the network's inherent porosity so larger-size molecules can pass. It is likely also that the opening and closing of a slit would be easier for the bacterium to control against random fluctuations than some other kind of aggregate structure. An example of the latter is shown in Fig. 1E, where a substantial opening can be created simply by moving the short isolated length of glycan strand (Fig. 1E). These openings could oscillate like flaps, opening and closing due to thermal fluctuations in the periplasm. It may be possible too that slits could be an easily recognizable physical marker for autolysins, so that these enzymes could machine larger transient holes for larger molecules.

It has recently been proposed that the sacculus expands (and the cell grows) by excising one old peptidoglycan strand and adding three new strands (Höltje's three-for-one hypothesis [7, 8]). This is an attractive idea, but there is a difficulty in that a bacterium must (somehow) be aware of the lengths of the preexisting strands at the location of the insertion. If, however, the ends of the strands at insertion locations are correlated because they form the side of a slit, this ready-made site might be preferred.

We have chosen not to calculate quantities such as the elasticity of the system, since there are a number of unknowns, including the spring energy of the septapeptide, octapeptide, or nonapeptide cross-links, the permissible range of the angles α and ψ shown in Fig. 4A, and the bending energy of the glycan strands. These questions have been addressed by Boulbitch (private communication), who has carried out a calculation of the elasticity of a peptidoglycan network without holes and other defects. This paper is concerned with deducing the hole structure that exists in gram-negative murein sacculi, subject to the constraint of the glycan strand length distribution. As described above, the presence of such slits could be advantageous for the bacterium, and this makes it an attractive model. At the present time we do not know of any physical or chemical method to validate our model. All attempts to visually detect specifically labeled slits by transmission electron microscopy (TEM) and metal decoration have failed because of moire effects as a result of superpositioned layers. Neutron or X-ray sources cannot be used to detect the slits as defects in a continuous network, since it is not yet possible to stack and orient sacculi with enough of the networks in register for suitable diffraction or reflection. It may be possible to supersede the moire problems inherent in TEM by using the enhanced imaging qualities of TEM-electron spectroscopic imaging (3), and we are currently exploring this possibility.

APPENDIX

Consider two aggregates, which we call a_1 and a_2, with the set of distances $\{r_{ij}\}$ being those between the individual tesserae which make up the two aggregates and with i and j representing tesserae on a_1 and a_2, respectively. Then the two aggregates interact with each other via the energy $V(a_1, a_2, \{r_{ij}\})$. We chose the simplest mathematical form

possible that yielded spatial distributions of aggregates which were easily distinguished from each other. A "one-over-r_{ij}^4" interaction was sufficiently "hard" to achieve this while being "soft" enough to permit the aggregates to move around and relax their distribution on the network. We chose

$$V(a_1, a_2, \{r_{ij}\}) = V_0 \sum_i \sum_j {}^1\!/\!_{r_{ij}^4}$$

If V_0 is positive (negative), then the interaction is repulsive (attractive). Choosing a V_0 equal to 0 will result in a random distribution, as long as the density of aggregates is not too high (i.e., as long as the aggregates can find sufficient room between the other aggregates to move around and relax into an equilibrium distribution). It should be clear that the aggregates do not rotate—they undergo only lateral movement.

This work was supported by Natural Sciences and Engineering Research Council of Canada (NSERC) research grants to D.P., T.B., and M.J. and by a St. Francis Xavier University Council for Research grant to D.P. J.M. was supported through an NSERC Summer Research Scholarship. We also appreciate the help of the Canadian Institute for Advanced Research (CIAR) for support through grants for travel and workshops.

We appreciate the comments of the referees.

REFERENCES

1. **Beveridge, T. J.** 1999. Structures of gram-negative cell walls and their derived membrane vesicles. J. Bacteriol. **181:**4725–4733.
2. **Beveridge, T. J., and T. Jack.** 1982. The binding of an inert cationic probe to walls of *Bacillus subtilis*. J. Bacteriol. **149:**1120–1123.
3. **Beveridge, T. J., T. J. Popham, and R. M. Cole.** 1994. Electron microscopy, p. 42–71. *In* P. Gerhardt (ed.), Methods for general and molecular bacteriology. American Society for Microbiology, Washington, D.C.
4. **Binder, K. (ed.).** 1984. Applications of the Monte Carlo method in statistical physics. Springer-Verlag, Heidelberg, Germany.
5. **de Jonge, B.** 1989. Peptidoglycan synthesis during the cell cycle of *Escherichia coli*: structure and mode of insertion. Ph.D. thesis. University of Amsterdam, Amsterdam, The Netherlands.
6. **Demchik, P., and A. L. Koch.** 1996. The permeability of the wall fabric of *Escherichia coli* and *Bacillus subtilis*. J. Bacteriol. **178:**768–773.
7. **Höltje, J.-V.** 1998. Growth of the stress-bearing and shape-maintaining murein sacculus of *Escherichia coli*. Microbiol. Mol. Biol. Rev. **62:**181–203.
8. **Höltje, J.-V.** 1995. From growth to autolysis: the murein hydrolases in *Escherichia coli*. Arch. Microbiol. **164:**243–254.
9. **Ishidate, K., A. Ursinus, J.-V. Höltje, and L. Rothfield.** 1998. Analysis of the length distribution of murein glycan strands in *ftsZ* and *ftsI* mutants of E. coli. FEMS Microbiol. Lett. **168:**71–75.
10. **Koch, A. L., and S. W. Woeste.** 1992. The elasticity of the sacculus of *Escherichia coli*. J. Bacteriol. **174:**4811–4819.
11. **Labischinski, H., G. Barnickel, D. Naumann, and P. Keller.** 1985. Conformational and topological aspects of the three-dimensional architecture of bacterial peptidoglycan. Ann. Inst. Pasteur/Microbiol. **136A:**45–50.
12. **Labischinski, H., E. W. Goodell, A. Goodell, and M. L. Hochberg.** 1991. Direct proof of a "more than-single-layered" peptidoglycan architecture of *Escherichia coli* W7: a neutron small-angle scattering study. J. Bacteriol. **173:** 751–756.
13. **Nanninga, N., and C. L. Woldringh.** 1985. Cell growth, genome duplication, and cell division, p. 259–318. *In* N. Nanninga (ed.), Molecular cytology of *Escherichia coli*. Academic Press, Inc., London, England.
14. **Obermann, W., and J.-V. Höltje.** 1994. Alterations of murein structure and of penicillin-binding proteins in minicells from *Escherichia coli*. Microbiology **140:**79–87.
15. **Saxton, M. J.** 1990. The membrane skeleton of erythrocytes. A percolation model. Biophys. J. **57:**1167–1177.
16. **Saxton, M. J.** 1992. Gaps in the erythrocyte membrane skeleton: a stretched net model. J. Theor. Biol. **155:**517–536.
17. **Sleytr, U. B., and T. J. Beveridge.** 1999. Bacterial S-layers. Trends Microbiol. **7:**253–260.
18. **Verwer, R. W. H., N. Nanninga, W. Keck, and U. Schwarz.** 1978. Arrangement of glycan chains in the sacculus of *Escherichia coli*. J. Bacteriol. **136:** 723–729.
19. **Wientjes, F. B., C. L. Woldringh, and N. Nanninga.** 1991. Amount of peptidoglycan in cell walls of gram-negative bacteria. J. Bacteriol. **173:**7684–7691.
20. **Yao, X., M. Jericho, D. Pink, and T. Beveridge.** 1999. Thickness and elasticity of gram-negative murein sacculi measured by atomic force microscopy. J. Bacteriol. **181:**6865–6875.